

Postcatalytic spliceosome structure reveals mechanism of 3'-splice site selection

Max E. Wilkinson,* Sebastian M. Fica, Wojciech P. Galej,† Christine M. Norman, Andrew J. Newman, Kiyoshi Nagai*

Introns are removed from eukaryotic messenger RNA precursors by the spliceosome in two transesterification reactions—branching and exon ligation. The mechanism of 3'-splice site recognition during exon ligation has remained unclear. Here we present the 3.7-angstrom cryo-electron microscopy structure of the yeast P-complex spliceosome immediately after exon ligation. The 3'-splice site AG dinucleotide is recognized through non-Watson-Crick pairing with the 5' splice site and the branch-point adenosine. After the branching reaction, protein factors work together to remodel the spliceosome and stabilize a conformation competent for 3'-splice site docking, thereby promoting exon ligation. The structure accounts for the strict conservation of the GU and AG dinucleotides at the 5' and 3' ends of introns and provides insight into the catalytic mechanism of exon ligation.

Pre-messenger RNA (pre-mRNA) splicing is catalyzed by a dynamic molecular machine called the spliceosome (1), which uses a single RNA-based active site (2, 3) to catalyze two sequential transesterification reactions that excise noncoding introns from pre-mRNA and ligate the coding exons to form mature mRNA. Introns are marked by GU and AG dinucleotides at the 5' and 3' splice sites (SS), respectively, and a branch point (BP) adenosine upstream of the 3'SS; these nucleotides are invariant except in introns removed by the metazoa-specific minor spliceosome (4). The spliceosome assembles de novo on each pre-mRNA by the ordered joining of five small nuclear ribonucleoprotein particles (snRNPs) and the NineTeen and NineTeen-Related (NTC and NTR) protein complexes, along with additional protein factors (1). First, the U1 and U2 snRNPs recognize the 5'SS and BP sequences of the pre-mRNA, respectively, forming A complex. Next, the preassembled U4/U6.U5 tri-snRNP joins to form pre-B complex, followed by spliceosome activation via B complex to form B^{act} complex. Subsequent Prp2-mediated remodeling yields B* complex, which is competent to carry out the first transesterification reaction, called branching, when the 2' hydroxyl of the conserved BP adenosine in the intron performs a nucleophilic attack on the 5'SS, producing the cleaved 5' exon and a branched lariat intron intermediate. The resulting C complex is then remodeled to C* complex upon dissociation of step 1 (branching) factors by the DEAH-box adenosine triphosphatase (ATPase) Prp16 (5, 6). In C* complex, step 2 (exon ligation) factors promote docking of the 3'SS into the active site (7) and

exon ligation, via nucleophilic attack of the 3' hydroxyl of the 5' exon at the 3'SS. The resulting P complex contains ligated exons (mRNA) and the excised lariat intron. The newly formed mRNA is then released from P complex by the DEAH-box ATPase Prp22 (8), forming the intron-lariat spliceosome (ILS), which is disassembled by the DEAH-box ATPase Prp43 (1) to recycle the snRNPs for further rounds of splicing.

Recent cryo-electron microscopy (cryo-EM) studies of yeast (6, 9–15) and human spliceosomes (16, 17) have elucidated the configuration of the RNA-based active site and many mechanistic details of splice site recognition and catalysis, as well as the role of specific protein factors (18). Structures of C complex (6, 12) showed how the spliceosome recognizes and positions the 5'SS and BP sequences in the active site through RNA-RNA interactions with U6 snRNA and U2 snRNA, while the branching factors Cwc25, Yju2, and Isy1 lock these sequences in a conformation competent for catalysis. Structures of C and C* complex (6, 14–17) revealed how Prp16 remodels the spliceosome into the exon ligation conformation, which is stabilized by the exon ligation factors Prp18 and Slu7 (7, 19, 20). In both C and C* complexes, the 5'SS and 5' exon remain paired with U6 snRNA (21, 22) and loop 1 of the U5 snRNA (23, 24), respectively. However, in the C*-complex structures, the 3' exon and 3'SS are not yet docked into the active site. Thus, it has remained unclear how the spliceosome selects and docks the 3'SS while aligning the 3' exon for step 2 catalysis. Additionally, it was not known how Slu7 and Prp18 interact with the 3'SS to promote docking.

Here, we report the cryo-EM structure of the *Saccharomyces cerevisiae* postcatalytic P complex at near-atomic resolution, showing the catalytic step 2 configuration of the active site. The structure reveals how the 3'SS and 3' exon are recognized by the spliceosome and shows the

critical role of the branched lariat intron in promoting the chemistry of exon ligation.

Overall architecture of P complex

We produced P complex by an in vitro splicing reaction supplemented with dominant-negative mutant Prp22 protein to prevent mRNA release from the spliceosome (25). Complexes with a docked 3' exon were selectively purified via MS2-MBP (maltose-binding protein) fusion protein. The resulting spliceosomes contained spliced mRNA and excised intron and were enriched in Prp22, as expected (fig. S1). We obtained a cryo-EM reconstruction at 3.7 Å overall resolution and modeled 45 components (figs. S2 and S3 and tables S1 and S2).

P complex has the same overall exon ligation conformation as C* complex (Fig. 1A). Relative to the branching conformation of C complex (6, 12), the branch helix between the intron and U2 snRNA has rotated 75° out of the active site, extracting the BP adenosine and creating space for the incoming 3' exon in the active center (Fig. 1, B and C, and Fig. 2, A and B). Branch helix rotation is accompanied by movement of the U2 snRNP and its attached NTC protein Syf1, and Prp16-mediated release of the branching factors Cwc25, Isy1, and the N-terminal domain of Yju2 (14, 15) (fig. S4A). The undocked branch helix is stabilized in its new position by the WD40 domain of Prp17 and by the Prp8 ribonuclease H (RNaseH) domain, which has rotated to insert its β hairpin near the BP (14, 15). The exon ligation factors Prp18 and Slu7 occupy the same locations as they do in C* complex, with the α-helical domain (26) of Prp18 binding the outer surface of the Prp8 RNaseH domain (Fig. 1C). Whereas in C* complex we could only assign the C-terminal globular domain of Slu7, the higher-quality density in P complex allowed us to essentially complete this model, revealing a sprawling architecture that spans 120 Å of the spliceosome (Fig. 1A). Prp22, which replaces Prp16 in both C* and P complex, is stabilized onto the Prp8 N-terminal domain through interactions with the C terminus of Yju2.

RNA active site

The RNA catalytic core of the P complex spliceosome remains essentially unchanged compared to C* complex (14–17) (Fig. 2, A and B), except that the 3' exon is ligated to the 5' exon and the 3'SS is docked into the space occupied by the branch helix in C complex (Figs. 1, B and C, and 2B and fig. S3). The catalytic triplex formed by U2 and U6 snRNAs, harboring the catalytic metal ions, is unaltered (2, 3, 27), and the 5' exon remains base-paired to loop 1 of U5 snRNA (23, 24). The position of the 3'SS relative to the 3' exon suggests that prior to exon ligation, the pre-mRNA undergoes an almost 180° turn to expose the 3'SS scissile phosphate for nucleophilic attack by the 3' hydroxyl of the 5' exon. This deformation is similar to that seen during branching, when the 5'SS is highly bent to expose the scissile phosphate to the BP adenosine nucleophile (6, 12) (fig. S5).

MRC Laboratory of Molecular Biology, Francis Crick Avenue, Cambridge CB2 0QH, UK.

*Corresponding author. Email: mwilkin@mrc-lmb.cam.ac.uk

(M.E.W.); kn@mrc-lmb.cam.ac.uk (K.N.) †Present address:

European Molecular Biology Laboratory (EMBL) Grenoble, 71 Avenue des Martyrs, 38042 Grenoble Cedex 09, France.

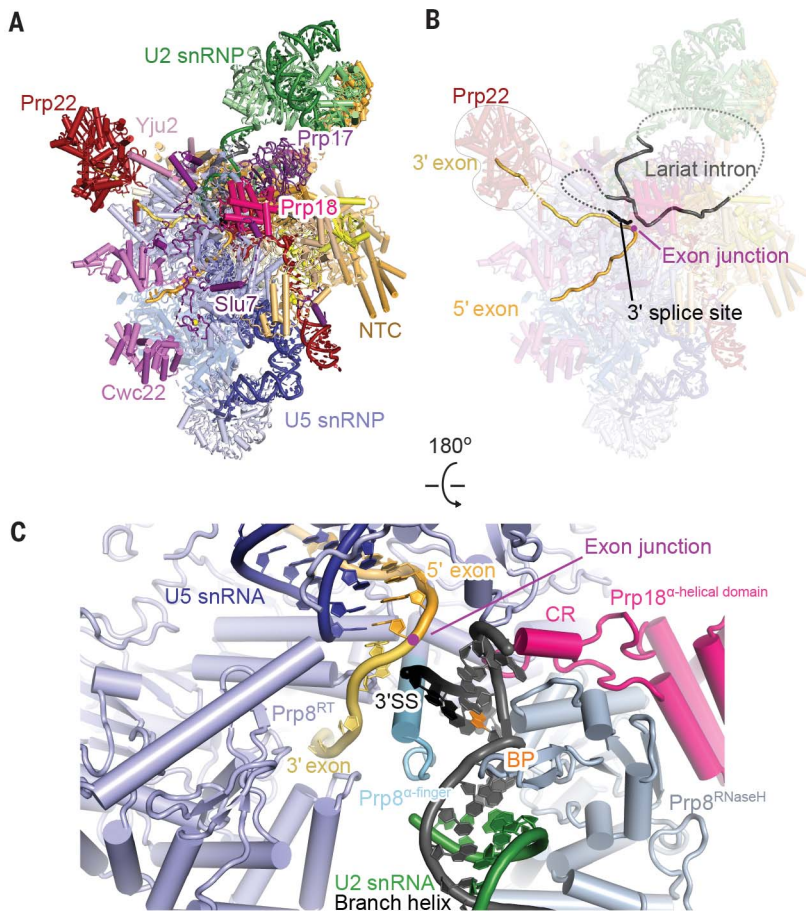


Fig. 1. P-complex structure. (A) Overview of the P-complex spliceosome. NTC, NineTeen complex. (B) The same view of P complex with the path of the substrate intron and exons shown. Dotted lines indicate the path of nucleotides not visible in the density. (C) Binding of substrate at the core of P complex. U6 snRNA, NTC, and NTR proteins are omitted for clarity. 3'SS, 3' splice site; RT, Prp8 reverse transcriptase domain; CR, Prp18 conserved region.

The first two bases of the 3' exon are well ordered and extend the 5' exon with A-form helical geometry and regular base stacking (Fig. 2D), whereas 10 nucleotides of the 5' exon are well ordered in the channel between the N-terminal and large domains of Prp8. Density for the 3' exon downstream of G(+2) becomes weaker and follows the surface of the Prp8 reverse transcriptase (RT) domain up toward Prp22 (fig. S3F), consistent with cross-linking experiments (25). This arrangement is consistent with the role of Prp22 in pulling the ligated exon from the 3' direction to release mRNA (25). Our C-complex structure revealed a similar mechanism for remodeling by Prp16 (6, 18). It was previously shown that U5 snRNA loop 1 aligns the 5' exon and 3' exon for ligation (23, 24). Indeed, U5 snRNA U96, which points away from the active site in B^{act}, C, and C* complexes, can pair with G(-1) of the 5' exon in P complex (Fig. 2E), explaining previous genetic and cross-linking data (23, 24).

In yeast, the intron sequence of the 3'SS immediately preceding the 3' exon is stringently

conserved as Y(-3)A(-2)G(-1), where Y is any pyrimidine (28) (fig. S6A). In our P-complex structure, the phosphodiester bond at the 3'SS is cleaved, but the 3' hydroxyl of the 3'SS nucleotide G(-1) remains close to the phosphate of the newly formed exon junction, consistent with observations that exon ligation is reversible (29) (Fig. 2D). This suggests that our structure represents the state of the spliceosome immediately after exon ligation, allowing us to infer the mechanism of 3'SS recognition (Fig. 2, C and F). Notably, the Hoogsteen edge of the 3'SS G(-1) forms a base pair with the Watson-Crick edge of the 5'SS G(+1), while stacking on U6 snRNA A51, which remains paired to U(+2) of the 5'SS (24) as in C* complex (14). This arrangement allows the 3' hydroxyl of 3'SS G(-1) to project toward the active site (Fig. 2D). The Hoogsteen edge of the 3'SS A(-2) interacts with the Hoogsteen edge of the BP adenosine, which is still linked via its 2' hydroxyl to the 5'SS G(+1). Thus, 3'SS recognition is achieved through RNA base-pairing with the 5'SS and the BP adenosine. This mech-

anism is consistent with the genetic interactions between the first and last bases of the intron (30, 31) and exon ligation defects observed in BP mutants (32, 33) (fig. S6). Notably, mutations at 3'SS G(-1) that are proofread and undocked by Prp22 (7) would destabilize the interaction between the 5'SS and the 3'SS (fig. S6), consistent with a proofreading mechanism in which Prp22 senses the stability of the docked 3'SS (7), although the structural basis for such sensing remains unknown. We additionally observed ordered density for 3'SS nucleotides (-3) to (-5), whereas the 20 nucleotides connecting the 3'SS to the branch helix were not visible and are likely disordered as they would loop out of the spliceosome from the branch helix to just upstream of the 3'SS.

Additional density adjacent to the 3' hydroxyl of 3'SS G(-1) was putatively interpreted as the catalytic Mg²⁺ M2 because it is coordinated by phosphate oxygen ligands from U6 snRNA bases U80, A59, and G60, which were previously shown biochemically to bind M2 (2). In contrast, no density consistent with M1 was observed, as expected for P complex being in a postcatalytic state, whereas M1 was predicted to coordinate the nucleophile in the precatalytic state and density consistent with M1 was indeed visible in C* complex (14) (figs. S3 and S5).

Proteins around the active site

Compared to C* complex, which lacked the docked 3' exon and 3'SS, new protein density is visible around the P-complex active site. Prp8 and Prp18 cooperate to stabilize the docked 3' splice site as well as the binding of the 3' exon (Fig. 3A). The 3' exon is sandwiched between the α finger and the reverse transcriptase domains of Prp8 (Fig. 1C) (34). The α finger (residues 1565 to 1610) of Prp8 forms an extended helix that wedges between the 3' exon and 3'SS (Fig. 3, B and C, and fig. S4). Before exon ligation, the contiguous 3' exon and 3'SS would wrap around this helix, exposing the 3'SS phosphate for attack by the 5' exon (Fig. 3B and fig. S5). α -Finger residue Arg¹⁶⁰⁴, which is essential for exon ligation (Fig. 3D and fig. S7), contacts the phosphate backbone of the 3'SS residues -3 and -4. The highly conserved Gln¹⁵⁹⁴ forms a hydrogen bond with the O2 carbonyl group of U(-3), and cytosine at the (-3) position could form an equivalent hydrogen bond, explaining the preference for pyrimidines at (-3) of the 3'SS (Fig. 3C and fig. S6). The non-Watson-Crick RNA pairing between the BP, the 5'SS, and the 3'SS is reinforced by these sequences being clamped between the Prp8 α finger and the β hairpin of the Prp8 RNaseH domain (Fig. 3A). Consistent with the structure, mutations in the β hairpin suppress the exon ligation defects of mutations at 3'SS A(-2) and the BP (35), further underscoring the essential structural role of Prp8 in 3'SS docking. The so-called conserved region of Prp18 (26) forms a loop that penetrates from outside the spliceosome through a channel formed by Prp8 into the active site, where it buttresses against nucleotides U(-3) and C(-4) of the 3'SS (Figs. 1C and 3, A and B).

Deletion of this conserved loop in Prp18 affects 3'SS selection (36), consistent with its direct involvement in exon ligation.

Step 2 factors promote exon ligation

In C complex, the branching factors Cwc25, Isy1, and Yju2 make extensive contacts with the branch and ACAGAGA helices and together directly stabilize the docking of the distorted branch helix into the active site to allow efficient branching (6, 12). In P complex, the exon ligation factors Prp18 and Slu7 make only one direct contact with the active site RNA, via the Prp18 conserved loop (Fig. 3, A and B), whereas the α -helical domain of Prp18 binds the outer face of the Prp8 RNaseH domain (Fig. 4A). The N terminus of Slu7 binds to the Cwc22 C-terminal and Prp8 linker and endonuclease domains. Slu7 then extends to the Prp8 N-terminal domain, where it is anchored by its zinc-knuckle domain before passing through the interface between the Prp8 N-terminal and endonuclease domains. After a helical interaction with Prp18, the globular C-terminal region of Slu7

binds the inner surface of the Prp8 RNaseH domain (Fig. 4A). This mostly peripheral binding of exon ligation factors suggests that they promote splicing by a less direct mechanism than branching factors, which lock the branch helix in the active site.

Docked and undocked conformations of P complex

We performed global classification of our cryo-EM data set to assess the conformational dynamics of P-complex spliceosomes. A subset comprising approximately half of the purified P-complex particles lacks density for the 3'SS and Prp8 α finger (fig. S8). In this "undocked" conformation, the junction between the 5' exon and 3' exon in ligated mRNA is still visible, confirming that the undocked conformation represents a P-complex state. These particles also lack density for Prp18 and Slu7, indicating that the presence of exon ligation factors correlates with stable docking of the 3'SS (Fig. 4, B and C). This is consistent with previous biochemistry and genetics that suggest

that Slu7 and Prp18 act after Prp16-mediated remodeling (7, 37) and promote juxtaposition of the splice sites in the exon ligation conformation (7). The branch helix, which is locked in place by exon ligation factors in the docked conformation, undergoes slight movement together with Prp17 in the undocked conformation and has weaker density, suggesting that it is more flexible in the absence of exon ligation factors (Fig. 4, B and C, and fig. S8). Because the BP adenosine in the branch helix and the attached 5'SS G(+1) form the recognition platform for the 3'SS AG sequence, it is likely that the 3'SS can only stably dock when the branch helix is held rigid in the docked conformation.

The docked conformation competent for exon ligation is also associated with stronger density for two long collinear α helices spanning the width of the spliceosome from the C terminus of Syf1 to the Prp8 RNaseH domain and contacting Cef1 (Fig. 4C). This density was previously seen weakly in C* complex (14), but limited local resolution precluded its assignment. The higher

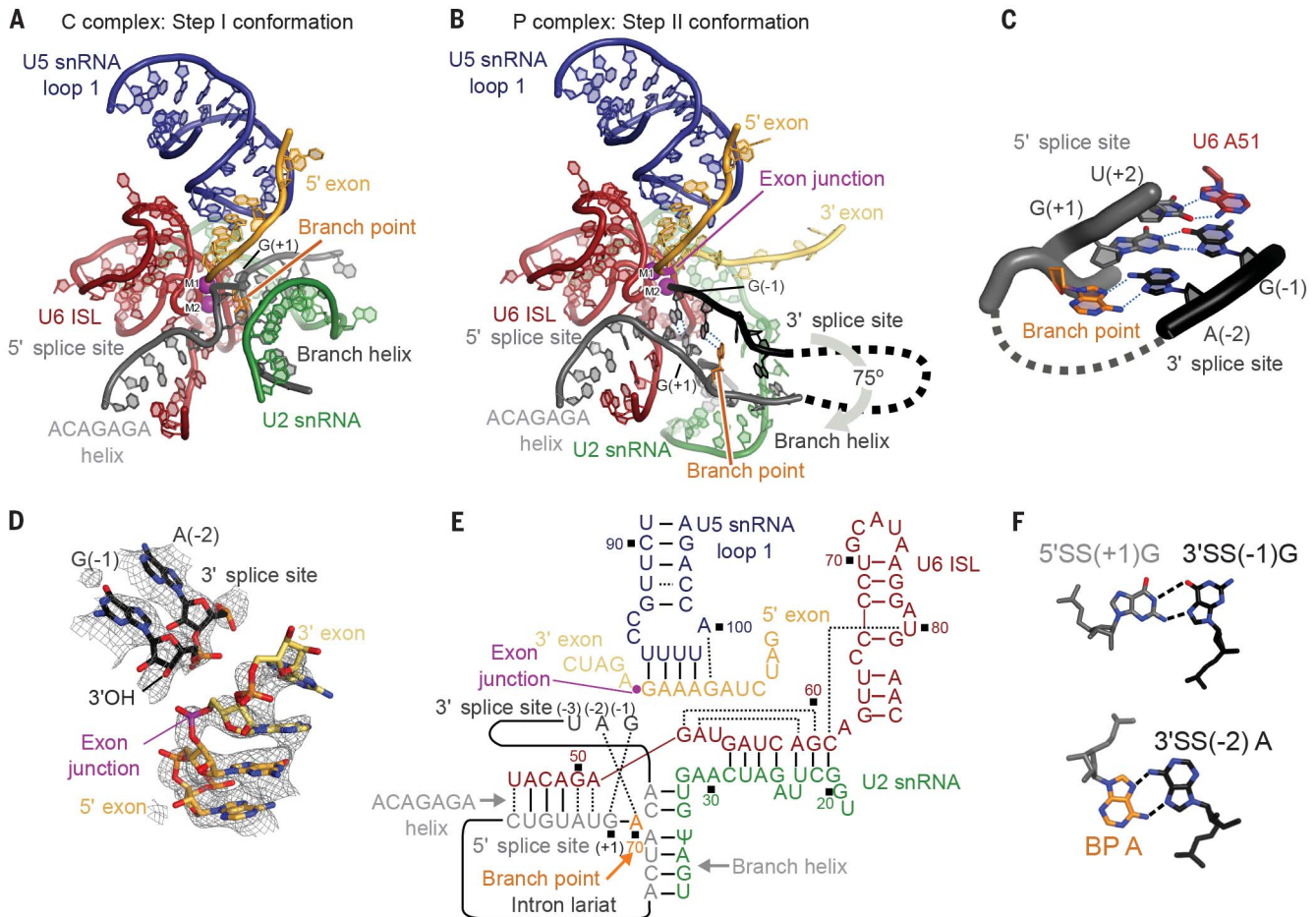
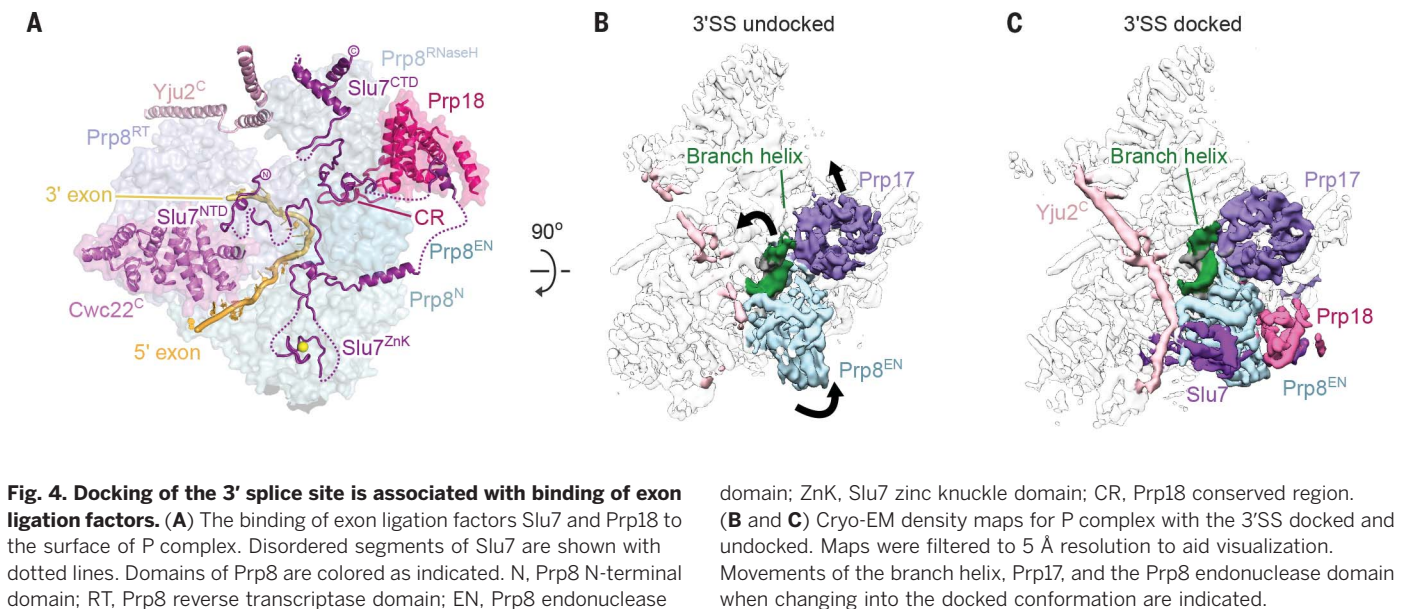
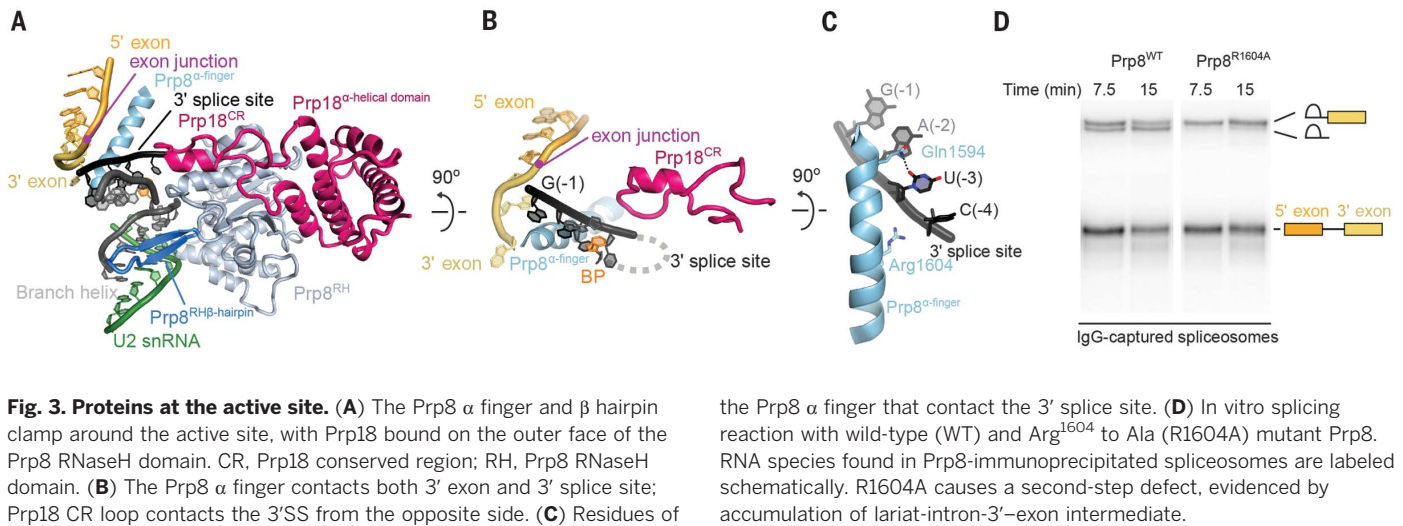


Fig. 2. Structure of the RNA catalytic core. (A) Key RNA elements at the active site of the C-complex spliceosome. ISL, internal stem-loop; M1 and M2, catalytic metal ions one and two. (B) Equivalent view to (A) of the active site of the P-complex spliceosome. M1 was not visible in the density, and its position is inferred from C and C* complexes. (C) Non-Watson-Crick RNA-RNA interactions mediate recognition of the 3' splice site. Putative hydrogen bonds

are shown with dotted blue lines. Branch point adenosine and U6 snRNA A51 are highlighted. (D) Cryo-EM density around the exon junction for the 5' exon, 3' exon and 3' splice site. (E) Base-pairing scheme of the P-complex active site. Watson-Crick pairing is indicated with lines, other base pairs with dotted lines. Ψ , pseudo-uridine. (F) Details of the pairing that mediates 3' splice site (3'SS) recognition. 5'SS, 5' splice site; BP A, branch-point adenosine.



quality of the P-complex density allowed assignment of these helices as the C terminus of Yju2. In contrast, the N terminus of Yju2 binds onto the branch helix and acts as a branching factor in C complex. However, the Yju2 N terminus is no longer visible in C* or P complexes. Previous experiments showed that the N-terminal and C-terminal domains of Yju2 can act in trans; the N-terminal domain is essential for branching but impedes exon ligation, whereas the C-terminal domain promotes exon ligation, despite not being essential for viability (38). Our structure explains these apparently opposing roles of Yju2 and suggests that the C-terminal domain stabilizes binding of Prp22 and Slu7 and acts as a brace, further restricting flexibility in the docked conformation. Thus, Yju2 is both a branching and exon ligation factor, and Prp16-dependent remodeling of C complex effects an exchange of its stable binding to the spliceosome from the N-terminal to the C-terminal domain (Fig. 5).

The two alternative forms of P complex suggest that exon ligation factors aid exon ligation in part by stabilizing the docked conformation: Prp18 and Slu7 bind together to the Prp8 RNaseH domain in its rotated conformation induced by Prp16 remodeling of C complex, while Slu7 anchors the RNaseH domain in place via multipronged interactions with the other domains of Prp8 (Fig. 5). Slu7 may also promote exon ligation by additional mechanisms. Slu7 is dispensable for exon ligation when the distance between the BP and 3'SS is less than nine nucleotides (19, 39), consistent with the seven ordered nucleotides that we see in P complex, which could be joined by two additional nucleotides. The intron region between the BP and the docked 3'SS would likely protrude from the spliceosome through an opening between the Prp8 RNaseH, linker, and RT domains. Intriguingly, the N terminus of Slu7 binds at the base of this opening (Figs. 1B and 4A) and truncation of the N terminus abol-

ishes the ability of Slu7 to promote exon ligation for pre-mRNAs with long BP-3'SS distances (37). Thus, the N terminus of Slu7 could reduce the entropic cost of 3'SS docking. In conjunction with Prp18, Slu7 could also guide the 3'SS into the active site and promote the correct topology for stable 3'SS docking.

Conclusions

The molecular mechanism of 3'SS recognition during the catalytic phase of pre-mRNA splicing had been elusive despite decades of functional studies. Our P-complex structure now shows that the 3'SS is recognized by pairing with the 5'SS and the BP adenosine. This interaction involves all invariant nucleotides (GU and AG) at the 5' and 3' ends of the intron and the invariant BP adenosine, making the exon ligation step a final quality check of the splicing reaction. Indeed, mutation of any of these invariant nucleotides impairs mRNA formation (40, 41). Thus, like the

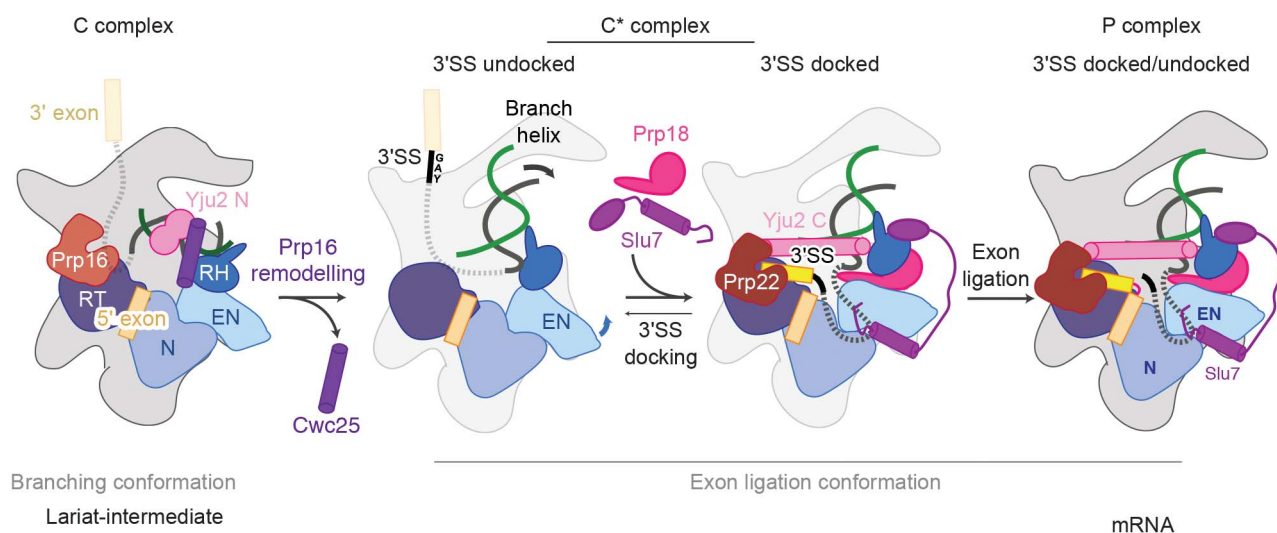


Fig. 5. Model for the action of exon ligation factors. After Prp16-mediated remodeling of C complex, the branching factors Cwc25, Yju2 N-domain, and Isy1 (not depicted) are removed. The undocked branch helix is then locked in a conformation competent for second-step catalysis

by the binding of exon ligation factors Prp18 and Slu7 and the C-domain of Yju2. The 3'SS docked and undocked conformations may be in equilibrium owing to flexibility of the branch helix and Prp8 endonuclease domain in the C* state.

5'SS GU dinucleotide and the BP A nucleotide, recognition of the 3'SS AG dinucleotide is achieved through non-Watson-Crick RNA-RNA interactions stabilized by protein factors, explaining the conservation of these splice site sequences throughout eukaryotic evolution. An AU at the 5'SS and an AC at the 3'SS—a combination observed in the human minor spliceosome (4) and as a suppressor of 5'SS mutations in yeast (30)—could also be tolerated (fig. S6), consistent with the major and minor spliceosome using a similar mechanism for 3'SS selection.

Although the structure of the RNA-based active site is markedly conserved between the spliceosome and group II self-splicing introns (fig. S5) (18, 42, 43), our P-complex structure reveals that specific recognition of the 3'SS differs between the two splicing systems. Whereas in the group II intron, the J2/3 junction interacts with the 3'SS (44), in the spliceosome, the equivalent region in U6 snRNA (nucleotide A51) interacts instead with the 5'SS to stabilize the C*- and P-complex configuration of the active site (Fig. 2B) (14). Nonetheless, in both systems, the 5'SS and the branch adenosine appear critical for both steps of splicing (Fig. 2) (43, 45), potentially explaining conservation of the 2'-5' linkage during evolution of both splicing systems.

Overall, our P-complex structure elucidates the mechanism of 3'-splice site selection, showing the crucial role of the excised lariat intron in organizing the active site and splice sites for exon ligation. The structure now completes our basic understanding of the two-step splicing reaction, showing how the dynamic protein scaffold of the spliceosome cradles and modulates a fundamentally RNA-based mechanism for splice site recognition during catalysis (18).

REFERENCES AND NOTES

1. M. C. Wahl, C. L. Will, R. Lührmann, *Cell* **136**, 701–718 (2009).

- S. M. Fica *et al.*, *Nature* **503**, 229–234 (2013).
- T. A. Steitz, J. A. Steitz, *Proc. Natl. Acad. Sci. U.S.A.* **90**, 6498–6502 (1993).
- A. A. Patel, J. A. Steitz, *Nat. Rev. Mol. Cell Biol.* **4**, 960–970 (2003).
- B. Schwer, C. Guthrie, *Nature* **349**, 494–499 (1991).
- W. P. Galej *et al.*, *Nature* **537**, 197–201 (2016).
- D. R. Semlow, M. R. Blanco, N. G. Walter, J. P. Staley, *Cell* **164**, 985–998 (2016).
- M. Company, J. Arenas, J. Abelson, *Nature* **349**, 487–493 (1991).
- C. Yan *et al.*, *Science* **349**, 1182–1191 (2015).
- C. Yan, R. Wan, R. Bai, G. Huang, Y. Shi, *Science* **353**, 904–911 (2016).
- R. Rauhut *et al.*, *Science* **353**, 1399–1405 (2016).
- R. Wan, C. Yan, R. Bai, G. Huang, Y. Shi, *Science* **353**, 895–904 (2016).
- C. Plaschka, P.-C. Lin, K. Nagai, *Nature* **546**, 617–621 (2017).
- S. M. Fica *et al.*, *Nature* **542**, 377–380 (2017).
- C. Yan, R. Wan, R. Bai, G. Huang, Y. Shi, *Science* **355**, 149–155 (2017).
- K. Bertram *et al.*, *Nature* **542**, 318–323 (2017).
- X. Zhang *et al.*, *Cell* **169**, 918–929.e14 (2017).
- S. M. Fica, K. Nagai, *Nat. Struct. Mol. Biol.* **24**, 791–799 (2017).
- T. Ohrt *et al.*, *RNA* **19**, 902–915 (2013).
- C. K. Tseng, H. L. Liu, S. C. Cheng, *RNA* **17**, 145–154 (2011).
- C. F. Lesser, C. Guthrie, *Science* **262**, 1982–1988 (1993).
- S. Kandels-Lewis, B. Séraphin, *Science* **262**, 2035–2039 (1993).
- A. J. Newman, C. Norman, *Cell* **68**, 743–754 (1992).
- E. J. Sontheimer, J. A. Steitz, *Science* **262**, 1989–1996 (1993).
- B. Schwer, *Mol. Cell* **30**, 743–754 (2008).
- J. Jiang, D. S. Horowitz, R. M. Xu, *Proc. Natl. Acad. Sci. U.S.A.* **97**, 3022–3027 (2000).
- S. M. Fica, M. A. Mefford, J. A. Piccirilli, J. P. Staley, *Nat. Struct. Mol. Biol.* **21**, 464–471 (2014).
- M. Spingola, L. Grate, D. Haussler, M. Ares Jr., *RNA* **5**, 221–234 (1999).
- C. K. Tseng, S. C. Cheng, *Science* **320**, 1782–1784 (2008).
- R. Parker, P. G. Siliciano, *Nature* **361**, 660–662 (1993).
- B. G. Luukkonen, B. Séraphin, *EMBO J.* **16**, 779–792 (1997).
- H. Hornig, M. Aebi, C. Weissmann, *Nature* **324**, 589–591 (1986).
- D. S. McPheeters, *RNA* **2**, 1110–1123 (1996).
- W. P. Galej, C. Oubridge, A. J. Newman, K. Nagai, *Nature* **493**, 638–643 (2013).
- L. Liu, C. C. Query, M. M. Konarska, *Nat. Struct. Mol. Biol.* **14**, 519–526 (2007).
- L. B. Crotti, D. Baciková, D. S. Horowitz, *Genes Dev.* **21**, 1204–1216 (2007).
- S.-A. James, W. Turner, B. Schwer, *RNA* **8**, 1068–1077 (2002).

- T.-W. Chiang, S.-C. Cheng, *Mol. Cell Biol.* **33**, 1746–1755 (2013).
- A. Brys, B. Schwer, *RNA* **2**, 707–717 (1996).
- M. Aebi, H. Hornig, R. A. Padgett, J. Reiser, C. Weissmann, *Cell* **47**, 555–565 (1986).
- U. Vijayraghavan *et al.*, *EMBO J.* **5**, 1683–1695 (1986).
- M. Marcia, A. M. Pyle, *Cell* **151**, 497–507 (2012).
- A. R. Robart, R. T. Chan, J. K. Peters, K. R. Rajashankar, N. Toor, *Nature* **514**, 193–197 (2014).
- A. Jacquier, F. Michel, *J. Mol. Biol.* **213**, 437–447 (1990).
- M. Costa, H. Walbott, D. Monachello, E. Westhof, F. Michel, *Science* **354**, aaf9258 (2016).

ACKNOWLEDGMENTS

M.E.W. prepared the sample, made EM grids, collected and processed EM data, carried out model building, and refined the structure. S.M.F. suggested the RNaseH method, prepared Prp22, and assisted data acquisition. W.P.G. was involved in the early stage of the project. M.E.W., S.M.F., and K.N. analyzed the structure and drafted a manuscript. Mutagenesis and splicing assays were carried out by A.J.N. and C.M.N. The manuscript was finalized by M.E.W., S.M.F., and K.N. with input from all authors. K.N. initiated and coordinated the spliceosome project. We thank C. Sava, S. Chen, G. McMullan, G. Cannone, J. Grimmett, and T. Darling for smooth running of the EM and computing facilities; the mass spectrometry facility for help with protein identification; and the members of the spliceosome group for help and advice throughout the project. We thank J. Löwe, V. Ramakrishnan, D. Barford, and R. Henderson for their continuing support and C. Plaschka, P. C. Lin, C. Charenton, C. J. Oubridge, and L. Strittmatter for critical reading of the manuscript. The project was supported by the Medical Research Council (MC_U105184330) and European Research Council Advanced Grant (AdG-693087-SPLICE3D). M.E.W. was supported by a Cambridge-Rutherford Memorial PhD Scholarship; S.M.F. was supported by a Marie Skłodowska-Curie fellowship. Cryo-EM maps are deposited in the Electron Microscopy Data Bank under accession numbers EMD-3979 (3'SS docked) and EMD-3980 (3'SS undocked); atomic models are deposited in the Protein Data Bank under accession number 6EXN.

SUPPLEMENTARY MATERIALS

www.sciencemag.org/content/358/6368/1283/suppl/DC1
Materials and Methods
Figs. S1 to S8
Tables S1 and S2
References (46–66)
PyMOL Session

31 October 2017; accepted 9 November 2017
Published online 16 November 2017
10.1126/science.aar3729

Postcatalytic spliceosome structure reveals mechanism of 3'–splice site selection

Max E. Wilkinson, Sebastian M. Fica, Wojciech P. Galej, Christine M. Norman, Andrew J. Newman and Kiyoshi Nagai

Science **358** (6368), 1283–1288.

DOI: 10.1126/science.aar3729 originally published online November 16, 2017

Understanding splicing from the 3' end

The spliceosome removes introns from eukaryotic mRNA precursors and yields mature transcripts by joining exons. Despite decades of functional studies and recent progress in understanding the spliceosome structure, the mechanism by which the 3' splice site (SS) is recognized by the spliceosome has remained unclear. Liu *et al.* and Wilkinson *et al.* report the high-resolution cryo-electron microscopy structures of the yeast postcatalytic spliceosome. The structures reveal that the 3' SS is recognized through non-Watson-Crick base pairing with the 5' SS and the branch point, stabilized by the intron region and protein factors.

Science, this issue p. 1278, p. 1283

ARTICLE TOOLS

<http://science.sciencemag.org/content/358/6368/1283>

SUPPLEMENTARY MATERIALS

<http://science.sciencemag.org/content/suppl/2017/11/15/science.aar3729.DC1>

RELATED CONTENT

<http://science.sciencemag.org/content/sci/358/6368/1278.full>

REFERENCES

This article cites 65 articles, 25 of which you can access for free
<http://science.sciencemag.org/content/358/6368/1283#BIBL>

PERMISSIONS

<http://www.sciencemag.org/help/reprints-and-permissions>

Use of this article is subject to the [Terms of Service](#)